Far-field Pattern Evaluation for Magnetically-biased Graphene Resonators via Quasi-normal Modes

Stamatios Amanatiadis[1], Tadao Ohtani[2], Theodoros Zygiridis[3], Yasushi Kanai[4], and Nikolaos Kantartzis[1]

[1]Aristotle University of Thessaloniki, Thessaloniki GR-54124, Greece, {samanati,kant}@auth.gr
[2]1-17-134, Omachi, Asahikawa 070-0841, Japan, bytcg100@ybb.ne.jp
[3]University of Western Macedonia, Kozani GR-50100, Greece, tzygiridis@uowm.gr
[4]Niigata Institute of Technology, Kashiwazaki 945-1195, Japan, kanai@iee.niit.ac.jp

This paper demonstrates the far-field response of magnetically-biased graphene plasmonic resonators at THz frequencies by employing quasi-normal mode schemes. First, the eigenstates are normalized using a non-trivial procedure, accounting for the anisotropic nature of graphene's surface conductivity. Next, the scattered field is computed by means of the modal coefficients of the quasi-normal modes for a general incident plane-wave. Finally, the far-field reconstruction, derived analytically from the scattered fields, is successfully validated against results from a full-wave solver, exhibiting exceptional accuracy.

***Index Terms*—Eigenvalues and eigenfunctions, magnetic anisotropy, metasurfaces, terahertz radiation**

I. Introduction

THE continuous advancement of telecommunications has introduced novel electromagnetic frameworks, including the robust analysis of time-dependent devices. Such devices comprise materials whose properties can be dynamically controlled through external stimuli, such as magneto-electrostatic biases. This artificial modulation enables extraordinary functionalities, including frequency generation [1] and amplification effects [2]. Within this context, graphene emerges as an excellent candidate for time-varying geometries due to its inherent ability to significantly alter electromagnetic properties under the influence of an external bias field.

Owing to its remarkable reconfigurability, graphene is often incorporated into metasurface designs to enable time-varying capabilities [3]. Consequently, the efficient computation of graphene-based devices scattering properties is crucial for predicting and optimizing the performance of the resulting metasurfaces. On the other hand, the quasi-normal mode (QNM) decomposition is a valuable technique for characterizing the scattering properties of such geometries [4]. Unlike traditional full-wave analysis, the QNM simulation is independent of the excitation, thus, significantly improving computational efficiency. However, modeling graphene for an eigenvalue analysis requires alternative approaches due to the frequency-dependent nature of its surface conductivity. To address this issue, the auxiliary field methodology has been proposed, linearizing the eigenvalue problem and achieving highly accurate results [5].

In this paper, the QNMs of a magnetically-biased graphene scatterer are processed to reconstruct its far-field pattern; a critical step in designing optimal metasurfaces. First, the QNM normalization procedure for a planar scatterer with anisotropic properties is introduced. This formulation enables the accurate extraction of modal coefficients, which are essential for determining the scattered near-field. The latter is, then, used to compute the far-field pattern via standard near-to-far field transformation techniques. The proposed method is validated by comparing its results to those obtained from a full-wave solver, demonstrating excellent precision. Moreover, significant computational efficiency is achieved, as all procedures are analytically derived after simulating the QNMs over the desired frequency range.

II. Proposed QNM-based Reconstruction

Consider graphene as an infinitesimally thin surface lying on the xy-plane, characterized by its surface conductivity. A magnetostatic bias field, B_0, is applied perpendicularly to the material's surface, directed along the z-axis. Under these conditions, the surface conductivity of graphene is expressed in tensor form as:

$$\bar{\bar{\sigma}}_{\rm gr}(\omega) = \begin{bmatrix} \sigma_d(\omega) & -\sigma_o(\omega) \\ \sigma_o(\omega) & \sigma_d(\omega) \end{bmatrix}, \tag{1}$$

$$\sigma_d(\omega) = \frac{A_{\mu_c}(j\omega + 2\Gamma)}{(j\omega + 2\Gamma)^2 + \omega_c^2}, \quad \sigma_o(\omega) = \frac{A_{\mu_c}\omega_c}{(j\omega + 2\Gamma)^2 + \omega_c^2}, \tag{2}$$

A_{μ_c} is a frequency-independent term, ω_c represents the cyclotron frequency, and Γ is the scattering rate.

The extraction of QNMs for a magnetically-biased graphene scatterer can follow the methodology proposed in [5]. However, the appropriate post-processing required to evaluate the far-field pattern is non-trivial due to the non-reciprocal nature of graphene's anisotropic conductivity. Specifically, two different solutions must be extracted: one using $\bar{\bar{\sigma}}_{\rm gr}$ and the other using $\bar{\bar{\sigma}}_{\rm gr}^T$. Thus, the following electric field/surface current pairs are obtained: $(\tilde{\mathbf{E}}_m^{(r)}, \tilde{\mathbf{J}}_m^{(r)})$ and $(\tilde{\mathbf{E}}_n^{(l)}, \tilde{\mathbf{J}}_n^{(l)})$, respectively. Although these solutions share the same eigenvalues $\tilde{\omega}_m$, the components differ due to the non-reciprocity, i.e., $\tilde{\mathbf{E}}_m^{(l)} \neq \tilde{\mathbf{E}}_m^{(r)}$ and $\tilde{\mathbf{J}}_m^{(l)} \neq \tilde{\mathbf{J}}_m^{(r)}$. To address this, the generalized QNM normalization scheme on the graphene surface is defined as:

$$\iint_S \frac{A_{\mu_c}}{2}\left[\frac{\tilde{\mathbf{E}}_n^{(l)} \cdot \bar{\bar{S}}_1 \tilde{\mathbf{E}}_m^{(r)}}{(j\tilde{\omega}_m + 2\Gamma + j\omega_c)^2} + \frac{\tilde{\mathbf{E}}_n^{(l)} \cdot \bar{\bar{S}}_2 \tilde{\mathbf{E}}_m^{(r)}}{(j\tilde{\omega}_m + 2\Gamma - j\omega_c)^2}\right] {\rm d}S = \delta_{nm}, \tag{3}$$

where $\bar{\bar{S}}_1 = \begin{bmatrix} 1 & -j \\ j & 1 \end{bmatrix}$ and $\bar{\bar{S}}_2$ is its complex conjugate pair.

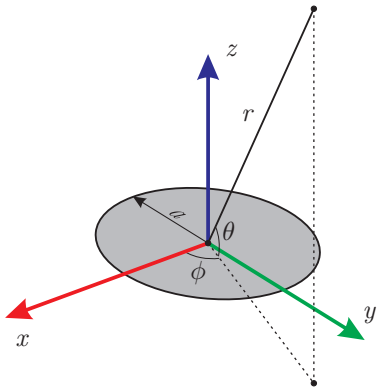


Fig. 1. Magnetic potential of a graphene disk scatterer at a point, expressed as a function of (r, θ, ϕ).

After applying the abovementioned normalization to the extracted eigenstates, the scattered surface current density on graphene is calculated as:

$$\mathbf{J}_{\mathrm{sc}}(\mathbf{r}, \omega) = \sum_m \alpha_m(\omega) \tilde{\mathbf{J}}_m^{(r)}(\mathbf{r}). \tag{4}$$

where $\alpha_m(\omega)$ stands for the modal coefficients, determined by the QNM surface current density $\tilde{\mathbf{J}}_m^{(r)}(\mathbf{r})$ and the electric field component of the incident plane wave. Finally, $\mathbf{J}_{\mathrm{sc}}(\mathbf{r}, \omega)$ is used to compute the vector magnetic potential at a given point R, expressed as a function of (r, θ, ϕ), as depicted in Fig. 1,

$$\mathbf{A}(r, \theta, \phi) = \frac{\mu_0}{4\pi} \iint_S \frac{\mathbf{J}_{\mathrm{sc}}(\mathbf{r}, \omega)}{R} \mathrm{e}^{-jkR} \mathrm{d}S, \tag{5}$$

where k is the wavenumber. The far-field evaluation can, then, be straightforwardly calculated using standard radiation pattern methods [6].

III. Numerical Validation

The proposed methodology is verified by comparing the analytically reconstructed far-field pattern from the QNMs with results obtained from full-wave analysis. Specifically, a graphene disk scatterer with a radius of $r = 40\,\mu$m is illuminated by an x-polarized plane wave propagating along the y-axis. The absorption cross-section, shown in Fig. 2, highlights the resonances and their corresponding surface current distributions. Notably, a gyrotropic pattern emerges, attributed to the anisotropic nature of graphene's surface conductivity. This is further confirmed by the normalized far-field pattern in Fig. 3, which shows maximum radiation at approximately 120° and 300°, indicating a 30° rotation relative to the incident wave direction. Moreover, the exceptional agreement between the reconstructed pattern from the QNMs and the full-wave results demonstrates the accuracy of the featured technique.

IV. Conclusion

An efficient method for far-field pattern reconstruction, integrated with the QNM framework, has been developed for magnetically biased graphene scatterers. The non-reciprocal characteristics of the anisotropic conductivity have been properly accounted for to evaluate the scattered surface current density on graphene, a key factor in determining the far-field pattern. The validity of the new scheme has been confirmed through comparisons with full-wave analysis, while its analytical nature significantly enhances the overall computational performance.

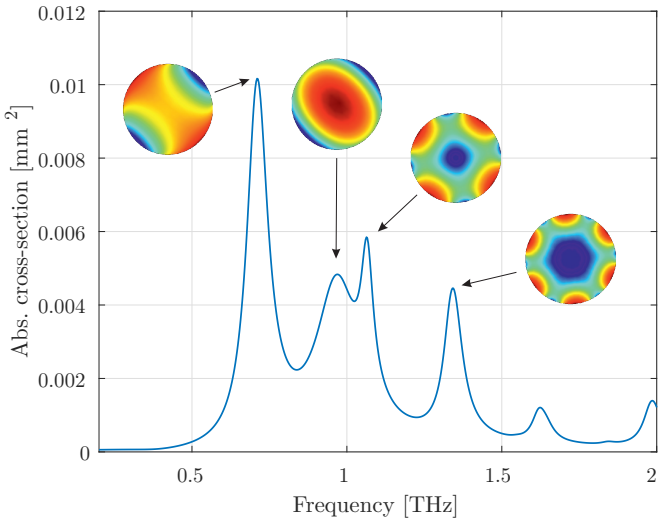


Fig. 2. Absorption cross-section of a graphene disk scatterer for an x-polarized incident plane wave propagating along the y-axis. The inset figures illustrate the QNMs at the peaks.

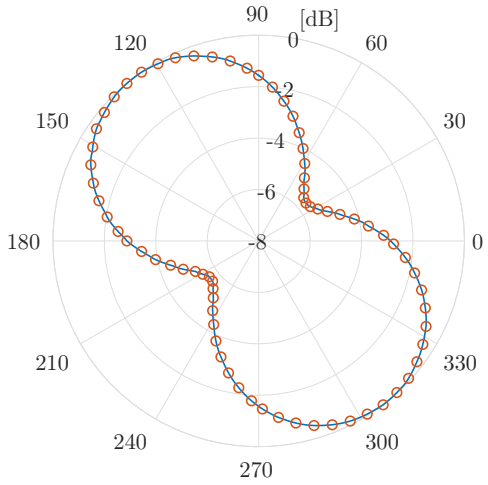


Fig. 3. Normalized far-field pattern on the xy-plane at 0.7 THz. The blue solid line represents the QNM-reconstructed pattern, while the red circles correspond to the results from the full-wave solver.

References

[1] J. Tunesi *et al.*, "Terahertz emission mediated by ultrafast time-varying metasurfaces," *Phys. Rev. Res.*, vol. 3, no. 4, pp. L042006, 2021.

[2] T. Koutserimpas, "Parametric amplification interactions in time-periodic media: coupled waves theory," *JOSA B*, vol. 39, no. 2, pp. 481–489, 2022.

[3] H. Rajabalipanah *et al.* "Reprogrammable spatiotemporally modulated graphene-based functional metasurfaces," *IEEE Trans. Emerg. Sel. Topics Circuits Syst.*, vol. 10, no. 1, pp. 75–87, 2020.

[4] W. Yan *et al.*, "Rigorous modal analysis of plasmonic nanoresonators," *Phys. Rev. B*, vol. 97, no. 20, pp. 205422, 2018.

[5] S. Amanatiadis *et al.*, "Effective finite-difference modeling of graphene micro-resonators for the accurate natural frequency extraction," *Phys. Rev. B*, vol. 60, no. 3, pp. 3313095, 2024.

[6] C. Balanis, *Antenna Theory: Analysis and Design*, John Wiley & Sons, New York, NY, 2015.